



# Application of Autoscala to ionograms recorded by the AIS-Parus ionosonde

I. Krasheninnikov<sup>b</sup>, M. Pezzopane<sup>a,\*</sup>, C. Scotto<sup>a</sup>

<sup>a</sup> Istituto Nazionale di Geofisica e Vulcanologia, Rome, Italy

<sup>b</sup> Pushkov Institute of Terrestrial Magnetism, Ionosphere and Radiowave Propagation, Russia

## ARTICLE INFO

### Article history:

Received 24 March 2009

Received in revised form

1 September 2009

Accepted 4 September 2009

### Keywords:

Ionogram

Ionosonde

Automatic scaling

Ionospheric monitoring

## ABSTRACT

Autoscala was applied to ionograms recorded by the digital AIS-Parus ionosonde, built at the Pushkov Institute of Terrestrial Magnetism, Ionosphere and Radiowave Propagation, Russia, and installed in Moscow (55.5N, 37.5E). Some results in regard to the reliability of the  $foF2$ ,  $foF1$ , and  $ftEs$  autoscaled characteristics are presented and discussed. The flexibility of Autoscala is illustrated based on its modular structure.

© 2010 Elsevier Ltd. All rights reserved.

## 1. Introduction

The ionosphere is the section of the Earth's atmosphere beginning at an altitude of about 50 km and extending outwards 2000 km or more. This region consists of layers of free electrically charged particles that transmit, refract, and reflect HF radio waves.

The ionosphere is routinely monitored by swept frequency vertical sounding radars, called ionosondes. These radars transmit vertical pulses of radio waves of frequency  $f$  and measure the time-of-flight  $t$  which elapses before the echo is received.

The result of a sounding is presented as a graph of  $t$  against  $f$ , called an ionogram. Each ionospheric layer shows up in an ionogram as an approximately smooth curve, separated from the other layers by an asymptote corresponding to an inflection in the electron density profile. The critical frequency of each layer is scaled from the asymptote, and the virtual height of each layer is scaled from the lowest point on each curve. An electron density profile is also often derived from an ionogram. For example, Fig. 1 shows an ionogram with corresponding profile. Each cusp observed on the ionogram is due to a maximum in the electron density profile and a corresponding critical frequency can be defined.

In recent years a growing interest in real-time applications has resulted in an increasing need for immediate availability of good scaled data. For this reason, the Istituto Nazionale di Geofisica e Vulcanologia (INGV) developed a computer program called

Autoscala (Scotto and Pezzopane, 2002; Pezzopane and Scotto, 2004, 2005), for the automatic scaling of the main ionospheric characteristics and the real-time estimation of the electron density profile.

The digital AIS-Parus ionosonde (Gajdanskij et al., 1996), built at the Pushkov Institute of Terrestrial Magnetism, Ionosphere and Radiowave Propagation, Russia, and installed in Moscow (55.5N, 37.5E), was designed on the classical scheme, using a simple pulsed signal. High power emission ( $\sim 12$  kW) and large-sized antenna enable reception of ionospheric echo starting from 1 MHz. It includes a system for the manual processing of sounding data, which enables estimation of an entire set of ionospheric parameters by an operator, but it is not equipped with a tool to perform automatic scaling of the recorded trace in real-time operation. This work describes the application of Autoscala to the ionograms recorded by this ionosonde and the initial results evaluating the reliability of the  $foF2$ ,  $foF1$ , and  $ftEs$  autoscaled values.

## 2. Data input

Autoscala works using ionograms as input in the form of binary files with the extension RDF. The name of the ionogram file is *yyggglmm.rdf*, where *yy* are the last two digits of the year, *ggg* are the three digits for the calendar day, *l* is the letter that identifies the hour (see Table 1 of Pezzopane, 2004) and *mm* represents the minutes (ex. *08151b00.rdf*, where 08 are the last two digits of the year 2008, 151 is the calendar day, *b* is the hour 01, and 00 are the minutes). Every file has a header of 197 bytes, with the bytes between 1 and 6 representing the initial frequency

\* Corresponding author. Tel.: +39 6 51860525; fax: +39 6 51860397.  
E-mail address: michael.pezzopane@ingv.it (M. Pezzopane).

of the sounding (which cannot be smaller than 1 MHz), the bytes between 8 and 13 representing the final frequency of the sounding, the bytes between 15 and 19 representing the frequency step, and the remaining bytes parameters concerning the receiver settings, the signal processing algorithm and geophysical constants depending on the specific installation site. Following the header these files are structured in a certain number (depending on the monitoring frequency bandwidth) of records of 150 bytes, each record representing the sounding in height for a specific value of the frequency; the value of the first byte represents the energy reflected back towards the ground from a height of 90 km, byte 150 represents the energy reflected back towards the ground from a height of 760.5 km, such that the passage between two successive bytes of the record is equal to a step in height of 4.5 km. The time processing of Autoscala depends on different parameters. One of these is the height resolution. Numerical tests performed from early versions have shown that considering a height resolution equal to 4.5 km represents a good compromise between reliability of outputs and time calculation.

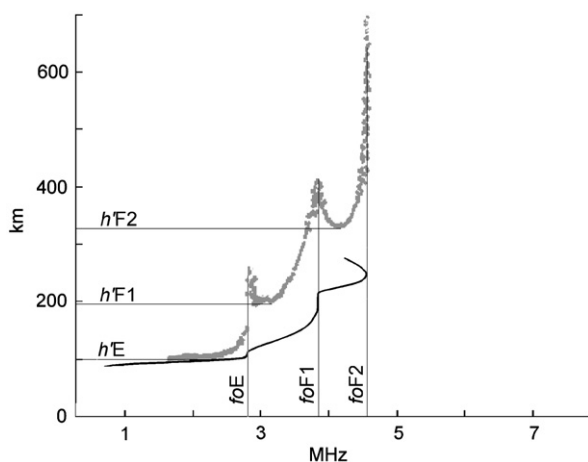


**Fig. 1.** An example of ionogram (in grey). Each maximum in the electron density profile (black line) leads to an asymptote observed on the ionogram in correspondence to which a critical frequency can be scaled. Virtual height of each layer is scaled from lowest point on corresponding curve.

In order to apply Autoscala to the ionograms recorded by the AIS-Parus ionosonde, a change of file format into RDF was required. The ionogram recorded by the AIS-Parus ionosonde is more detailed (the height resolution is about 2.4 km) than required by the RDF standard. In order to achieve this format change, the following simple principle was applied: for each pair of coordinates (frequency, virtual height) of the RDF, the nearest pair of coordinates of the original ionogram is identified and the corresponding value of amplitude is considered. An example of AIS-Parus ionogram conversion into RDF format is illustrated in Fig. 2 and it can be seen that the loss of information is limited.

### 3. Modular structure of Autoscala

Autoscala was developed with a modular structure comprising several routines designed to be tested and modified independently. With this modular structure, Autoscala can easily be adapted to particular ionograms and can also be integrated into new or existing structures.

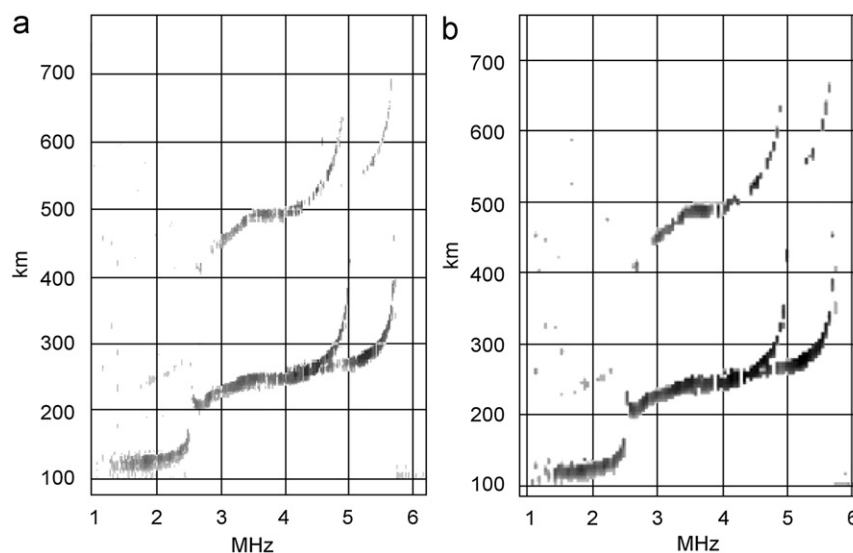
The kernel of the program is a routine for the automatic scaling of the critical frequency  $f_oF2$  and  $MUF(3000)F2$  from ionograms (Pezzopane and Scotto, 2007). Autoscala was later extended with the addition of a routine for the automatic scaling of the sporadic-E (Es) layer (Scotto and Pezzopane, 2007) and a routine for the F1 layer (Pezzopane and Scotto, 2008). Autoscala determines analytical functions for the F1 and F2 layers using an image recognition technique and can operate without polarization information. Autoscala was recently completed with the inclusion of a routine for real-time computation of the electron density profile (Scotto, 2009), which is essential for ionospheric monitoring and space weather applications.

Fig. 3 shows the flowchart of the algorithm of Autoscala. A brief description of the individual steps is given below.

#### 3.1. Ionogram acquisition and pre-processing

The raw ionogram recorded by the equipment is converted into a matrix whose dimensions are directly proportional to the frequency and height ranges, and inversely proportional to the frequency and height steps (Pezzopane and Scotto, 2008).

In order to achieve as clear a definition as possible, before being elaborated by the different modules of Autoscala, the



**Fig. 2.** (a) Ionogram recorded by AIS-Parus ionosonde on 02 February 2009 at 10:00 UT (b) after having been converted into RDF format.

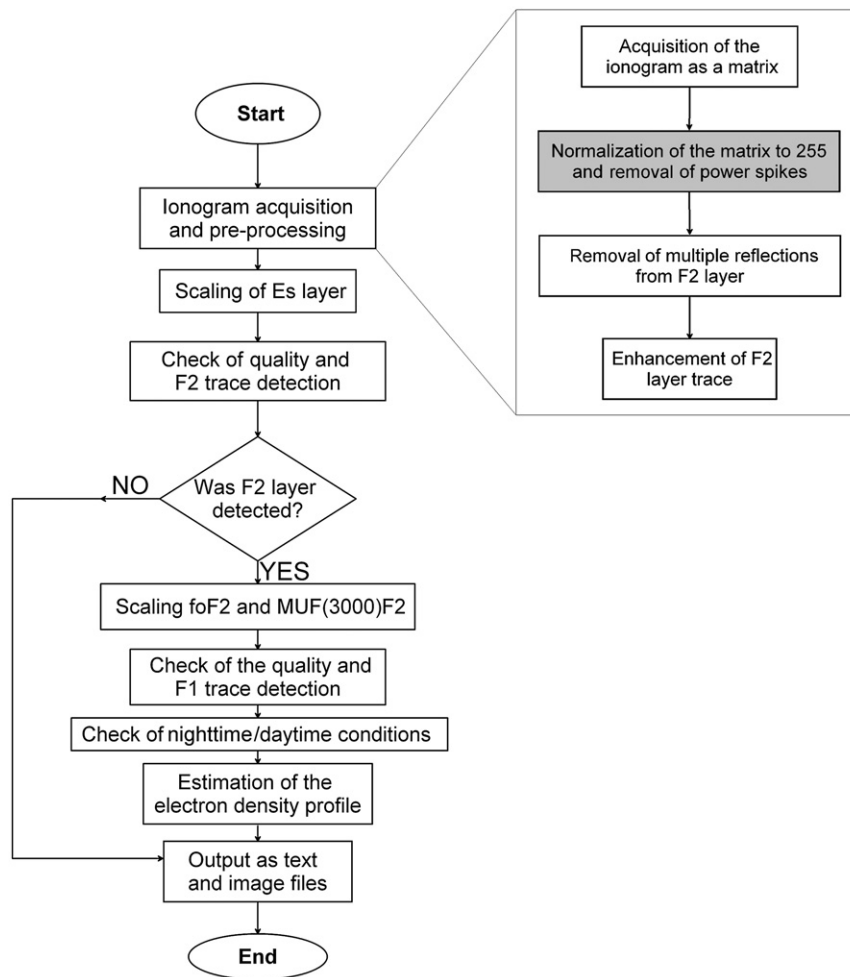


**Fig. 3.** Flowchart of algorithm of Autoscala in which “Ionogram acquisition and pre-processing” routine is expanded as a more detailed flowchart. Modular structure of Autoscala allowed modification of this routine by the addition of a routine to remove possible power spikes resulting from format change shown in Fig. 2.

ionogram trace is subjected to some pre-scaling processes, as described in §3.1.1 and §3.1.2.

### 3.1.1. Multiple reflections removal

A correlation-based filter is used to eliminate traces produced by second order reflection in the ionograms. This filter was developed (Scotto and Pezzopane, 2008) in order to smooth out cases in which the autoscaling of the ionogram was misled because second order F2 layer reflection was identified as first order reflection.

### 3.1.2. F2 trace highlighting

A linear regression-based filter is used to highlight the F2 ordinary and extraordinary rays in an ionogram. This filter was developed in order to smooth out cases in which the autoscaling of the ionogram was misled because the F2 ordinary ray was identified as the F2 extraordinary ray, with a consequent underestimation of the correct  $foF2$  value.

## 3.2. Scaling of Es layer

The first routine run by Autoscala is for the automatic interpretation of the Es layer and it establishes whether an Es layer is present or not. If an Es layer is identified, values for its maximum frequency  $ftEs$  and the associated virtual height  $h'Es$  are given as output.

## 3.3. Check of quality and F2 trace detection

After running the Es routine, the F2 routine runs and classifies the ionograms in one of the following three classes:

- (1) the trace is very clear and an operator would be able to easily scale  $foF2$  from the vertical asymptote;
- (2) the trace near the critical frequency is not clearly recorded owing to interference, absorption or scattering, but the trace can be reconstructed and a value of  $foF2$  extrapolated;
- (3) the trace is completely lost due to defects of the ionosonde or some ionospheric reasons.

For ionograms in class (1) the software limits itself to identifying the trace. For ionograms in class (3) the program establishes that the identification of the trace is not possible and consequently no output is produced.

As regards ionograms in class (2), Autoscala reconstructs the missing trace.

## 3.4. Scaling of $foF2$ and $MUF(3000)F2$

As fully described in the Appendix of Pezzopane and Scotto (2007), two empirical curves  $T_{ord}$  and  $T_{ext}$  that are able to fit the typical shape of the F2 trace are defined for the investigation of the ordinary and extraordinary ray. For each set of curves  $T_{ord}$  and

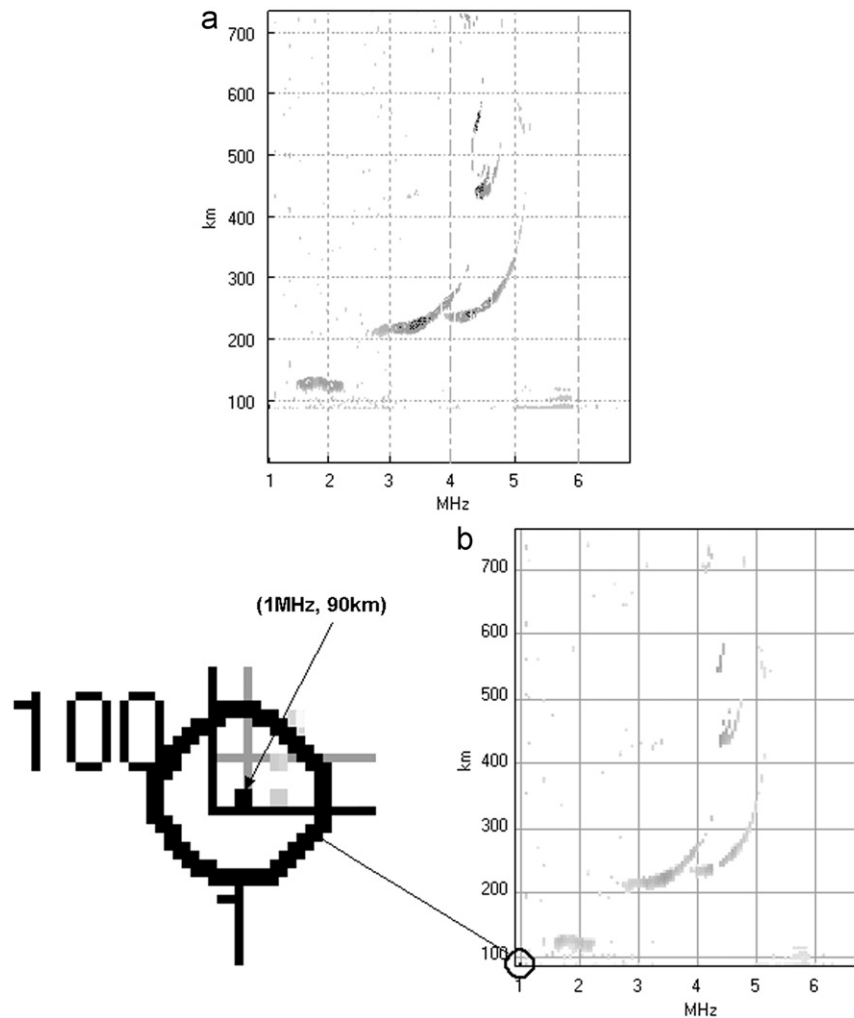


**Fig. 4.** (a) Ionogram recorded by AIS-Parus ionosonde on 01 January 2009 at 09:15 UT (b) after having been converted into RDF format. A power spike, highlighted by a black open circle on ionogram, is visible at point of coordinates (1 MHz, 90 km).

$T_{\text{ext}}$  the local contrast  $C$  with the recorded ionogram is calculated making allowance for both the number of matched points and their amplitude. The set of curves  $T_{\text{ord}}$  and  $T_{\text{ext}}$  having the maximum value of  $C$  is then selected. If this value of  $C$  is greater than a fixed threshold  $C_t$ , the selected curves are considered as representative of the F2 trace.  $foF2$  is thus obtained as the frequency of the vertical asymptote  $a_{\text{ord}}$  of  $T_{\text{ord}}$  while  $MUF(3000)F2$  is numerically calculated by finding the transmission curve tangent to  $T_{\text{ord}}$ . If  $C$  does not exceed  $C_t$ , the routine assumes the F2 trace is not present on the ionogram.

### 3.5. Check of nighttime/daytime conditions

The solar zenith angle  $\chi$  is calculated from the local time, geographical latitude and longitude. If  $\chi > 75^\circ$ , for winter months, or  $\chi > 87^\circ$ , for the rest of the year, then nighttime conditions are assumed and the search for the F1 cusp is not performed.

### 3.6. Check of quality and F1 trace detection

If an F2 trace was identified, the F1 routine runs and classifies the trace in one of the following three classes:

(1) the F1 cusp is clearly observable and an operator would be able to easily scale  $foF1$  from the vertical asymptote;

- (2) the trace is clear and an operator would be able to establish that the F1 layer is not present;
- (3) in the zone where the F1 cusp is expected the trace is missing due to defects of the ionosonde or some ionospheric reasons.

For the ionograms classified in set (1), Autoscala evaluates  $foF1$  from the vertical asymptote of the curve. For the ionograms classified in set (2), an output is given, informing the user that no F1 layer is observed. As regards the ionograms of set (3), the user is informed that the information is not sufficient to establish whether an F1 trace is present or not.

### 3.7. Electron density profile calculation

In this step the electron density profile is estimated using a model with 12 free parameters.

The 6 parameters related to the E region are: the maximum electron density  $NmE$ , the corresponding height  $hmE$ , the height of the valley point  $h\nu E$ , the valley width  $\delta h\nu E$ , the valley depth  $\delta N\nu E$ , and the layer semi-thickness  $ymE$ .

The 6 parameters related to the F2-F1 layers are: the maximum electron density  $NmF2$ , the corresponding height  $hmF2$ , the maximum electron density  $NmF1$ , the thickness parameter  $B0$ , and the shape parameters  $B1$  and  $D1$ .

In order to obtain the profile that best fits the recorded ionogram, an iterative technique is used to vary these parameters

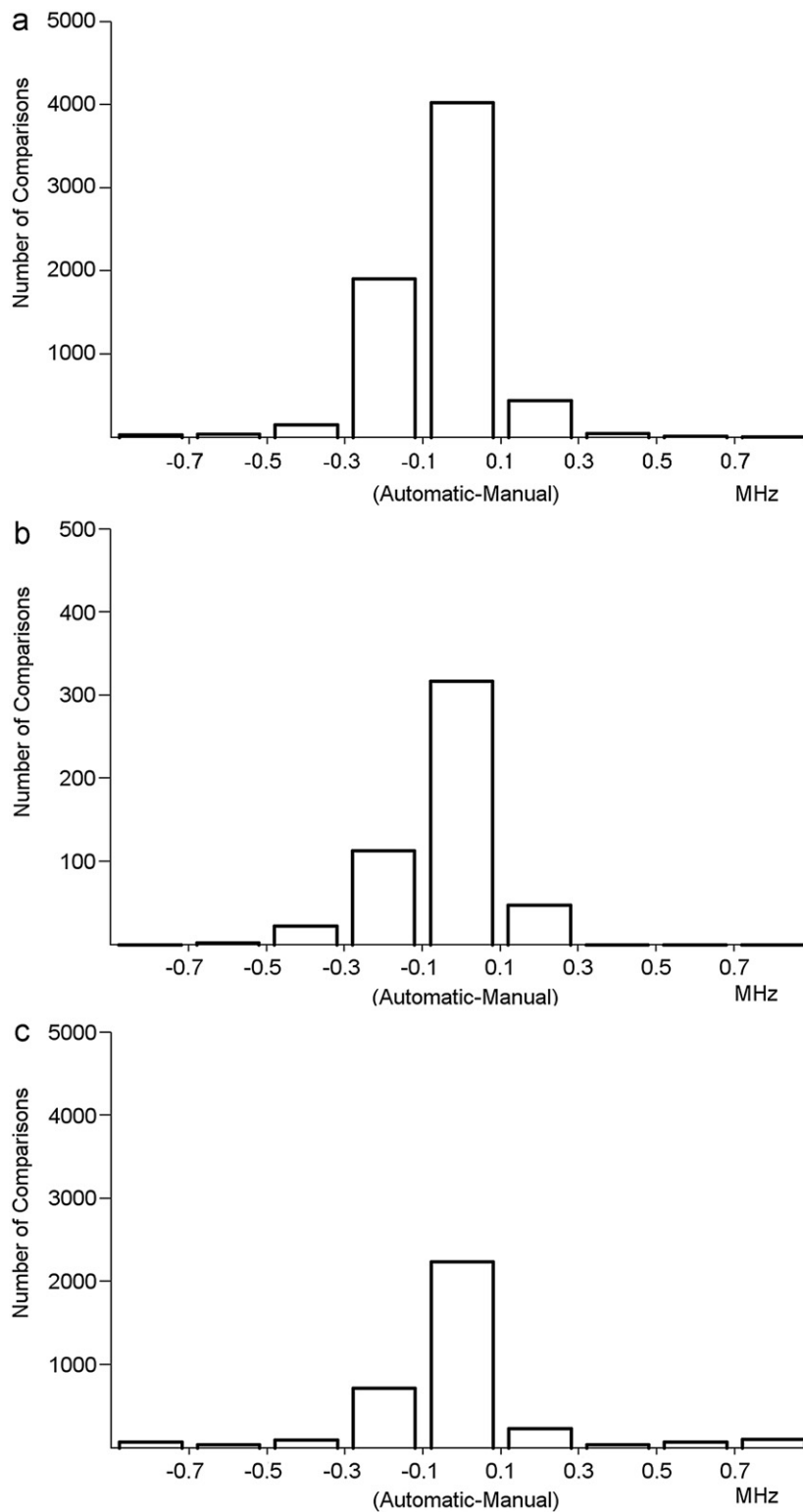


**Fig. 5.** (a) Differences ( $\delta = \text{Automatic} - \text{Manual}$ ) between values of  $foF2$  for ionograms for which both INGV software and operator identified the F2 layer. Out of 6654 cases results were: for 4030 cases ( $-0.1 \text{ MHz} \leq \delta \leq 0.1 \text{ MHz}$ ); for 418 cases ( $0.1 \text{ MHz} < \delta \leq 0.3 \text{ MHz}$ ); for 1904 cases ( $-0.3 \text{ MHz} \leq \delta < -0.1 \text{ MHz}$ ); for 66 cases ( $0.3 \text{ MHz} < \delta \leq 0.5 \text{ MHz}$ ); for 148 cases ( $-0.5 \text{ MHz} \leq \delta < -0.3 \text{ MHz}$ ); for 13 cases ( $0.5 \text{ MHz} < \delta \leq 0.7 \text{ MHz}$ ); for 38 cases ( $-0.7 \text{ MHz} \leq \delta < -0.5 \text{ MHz}$ ); for 7 cases ( $\delta > 0.7 \text{ MHz}$ ); for 30 cases ( $\delta < -0.7 \text{ MHz}$ ). (b) Differences ( $\delta = \text{Automatic} - \text{Manual}$ ) between values of  $foF1$  for ionograms for which both INGV software and operator identified the F1 layer. Out of 501 cases results were: for 317 cases ( $-0.1 \text{ MHz} \leq \delta \leq 0.1 \text{ MHz}$ ); for 47 cases ( $0.1 \text{ MHz} < \delta \leq 0.3 \text{ MHz}$ ); for 113 cases ( $-0.3 \text{ MHz} \leq \delta < -0.1 \text{ MHz}$ ); for 0 cases ( $0.3 \text{ MHz} < \delta \leq 0.5 \text{ MHz}$ ); for 22 cases ( $-0.5 \text{ MHz} \leq \delta < -0.3 \text{ MHz}$ ); for 0 cases ( $0.5 \text{ MHz} < \delta \leq 0.7 \text{ MHz}$ ); for 2 cases ( $-0.7 \text{ MHz} \leq \delta < -0.5 \text{ MHz}$ ); for 0 cases ( $\delta > 0.7 \text{ MHz}$ ); for 0 cases ( $\delta < -0.7 \text{ MHz}$ ). (c) Differences ( $\delta = \text{Automatic} - \text{Manual}$ ) between values of  $foEs$  for ionograms for which both INGV software and operator identified the Es layer. Out of 3591 cases results were: for 2235 cases ( $-0.1 \text{ MHz} \leq \delta \leq 0.1 \text{ MHz}$ ); for 231 cases ( $0.1 \text{ MHz} < \delta \leq 0.3 \text{ MHz}$ ); for 720 cases ( $-0.3 \text{ MHz} \leq \delta < -0.1 \text{ MHz}$ ); for 38 cases ( $0.3 \text{ MHz} < \delta \leq 0.5 \text{ MHz}$ ); for 92 cases ( $-0.5 \text{ MHz} \leq \delta < -0.3 \text{ MHz}$ ); for 66 cases ( $0.5 \text{ MHz} < \delta \leq 0.7 \text{ MHz}$ ); for 720 cases ( $-0.3 \text{ MHz} \leq \delta < -0.1 \text{ MHz}$ ); for 38 cases ( $0.3 \text{ MHz} < \delta \leq 0.5 \text{ MHz}$ ); for 92 cases ( $-0.5 \text{ MHz} \leq \delta < -0.3 \text{ MHz}$ ); for 66 cases ( $0.5 \text{ MHz} < \delta \leq 0.7 \text{ MHz}$ ); for 35 cases ( $-0.7 \text{ MHz} \leq \delta < -0.5 \text{ MHz}$ ); for 104 cases ( $\delta > 0.7 \text{ MHz}$ ); for 70 cases ( $\delta < -0.7 \text{ MHz}$ ).

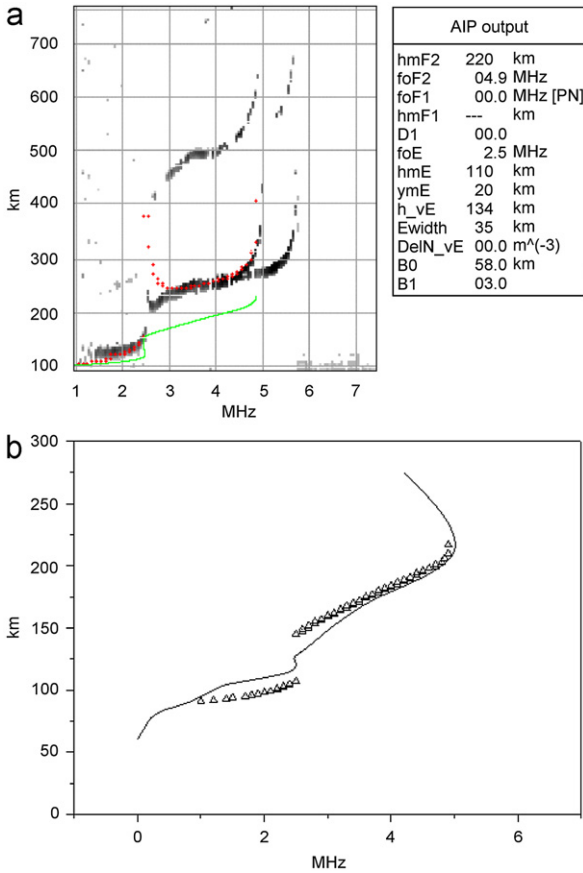


**Fig. 6.** (a) Ionogram recorded on 09 February 2009 at 10:00 UT and elaborated by Autoscala (in red the reconstructed ionogram and in green the corresponding electron density profile). On right, electron density profile parameters estimated by Autoscala. (b) Electron density profile calculated using POLAN (continuous line) after having manually digitized ionogram trace visible in (a) compared with electron density profile estimated by Autoscala (open triangle). (For interpretation of the references to colour in this figure legend, the reader is referred to the web version of this article.)

in a range centered on some “base values” calculated on the basis of the ionospheric characteristics obtained automatically from the ionograms by the routines previously described, and considering the helio-geophysical conditions (Scotto, 2009).

### 3.8. Output as text and image files

The output of the program is produced as TXT files suitable for data interchange and as GIF files for web page applications.

## 4. Adaptation of Autoscala to the AIS-Parus ionograms

In order to adapt Autoscala to the AIS-Parus ionosonde, some adjustments were necessary in the module in which data acquisition and pre-processing of ionograms are performed. In Fig. 3 the operations performed in this module are expanded as a more detailed flowchart.

Initially the ionogram is memorized by Autoscala as a matrix  $A$  of  $m$  rows and  $n$  columns. The element  $a_{ij}$  (with  $i=1, \dots, m$  and  $j=1, \dots, n$ ) of  $A$  is an integer proportional to the echo amplitude received by the ionosonde. This value is retrieved directly from the RDF file and it is then normalized setting to 255 the matrix element corresponding to the highest power recorded. For this reason the presence of a power spike makes the trace of the normalized ionogram unrealistically weaker (as is evident comparing Fig. 4b with Fig. 2b). Sometimes it may happen that after performing the ionogram file transformation described in Section 2, a few power spikes may be artificially introduced in the RDF ionogram file. Therefore, before the normalization routine, for the AIS-Parus ionograms it was necessary to add some lines of code to smooth out possible power spikes that could appear after conversion of the raw ionogram into RDF format, as illustrated in Fig. 4. In practice this smoothing consists in averaging all the entries  $a_{ij} \neq 0$  of the matrix  $A$

$$a_{med} = \frac{\sum_{i=1}^m \sum_{j=1}^n a_{ij}}{N} \tag{1}$$

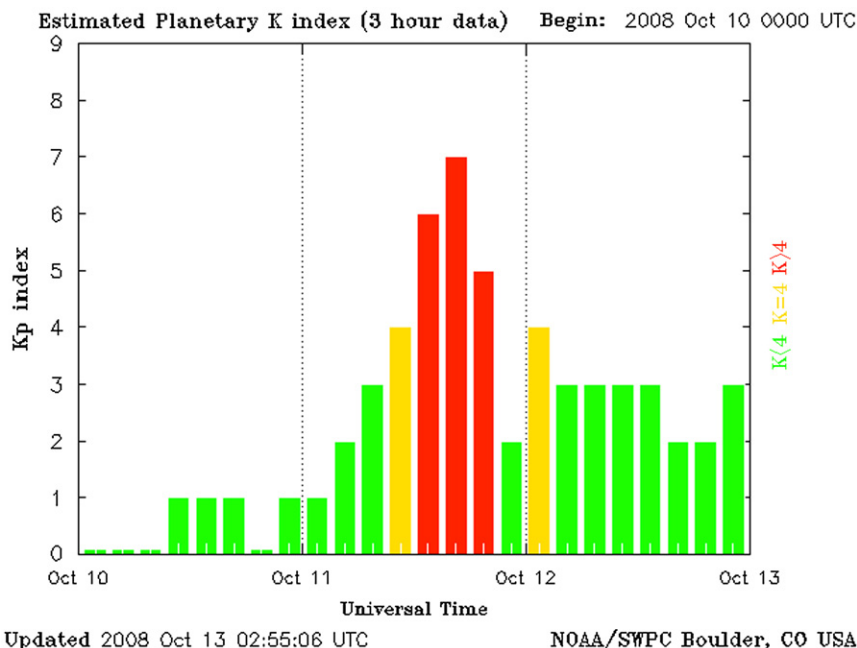


**Fig. 7.** Planetary K-indices plot downloaded from NOAA site (<http://www.swpc.noaa.gov/index.html>).

where  $N$  is the number of the entries  $a_{ij} \neq 0$ , and then in setting to  $a_{med}$  each element of the matrix  $A$  for which  $a_{ij} > 4a_{med}$ .

After introducing this modification in the pre-processing step, the ionograms were then real time transferred by ftp to a PC of the INGV on which Autoscala ran in the background. A web site (<http://ionos.ingv.it/Moscow/latest.html>) was also set up for testing.

## 5. A preliminary test

The performance of AIS-Parus and the Autoscala system was evaluated by testing the reliability of the  $foF2$ ,  $foF1$ , and  $ftEs$  autoscaled values using ionograms recorded from March to September 2008. The whole dataset consists of daytime and nighttime ionograms, recorded during quiet conditions, for which Autoscala considered the information sufficient to identify the layer (F2, F1, or Es), giving a value of the critical frequency ( $foF2$ ,  $foF1$ , or  $ftEs$ ) as output.

With regard to the ionograms discarded by Autoscala, the information was considered insufficient for identifying the layer trace because, for 98% of cases also the operator was not able to

observe the F2 trace for different reasons (absorption, interference, Es blanketing), for 89% of cases also the operator was not able to observe the F1 trace for the same reasons or because the F1 layer was really not present, and for 98% of cases also the operator was not able to observe the Es trace because it was really not present.

For the ionograms of the dataset, the values obtained automatically by Autoscala were compared with those obtained manually by a well-experienced operator according to the International Union of Radio Science (URSI) standard.

In this work a value is considered acceptable if within  $\pm 0.5$  MHz of the value obtained by the operator (such limits of acceptability have been adopted in line with the URSI limits of  $\pm 5\Delta$  where  $\Delta$  is the reading accuracy). The results are presented in the form of a histogram in Fig. 5a–c. The data analysis shows that  $foF2$ ,  $foF1$ , and  $ftEs$  values were acceptably scaled in a high percentage of cases (6566 out of 6654, equal to 98.7%, for  $foF2$ ; 499 out of 501, equal to 99.6%, for  $foF1$ ; 3316 out of 3591, equal to 92.3%, for  $ftEs$ ). The histograms reveal an asymmetrical distribution of errors which is a feature already observed in other analyses performed on ionograms recorded by different equipments (Pezzopane et al., 2008; Pezzopane and Scotto, 2004).

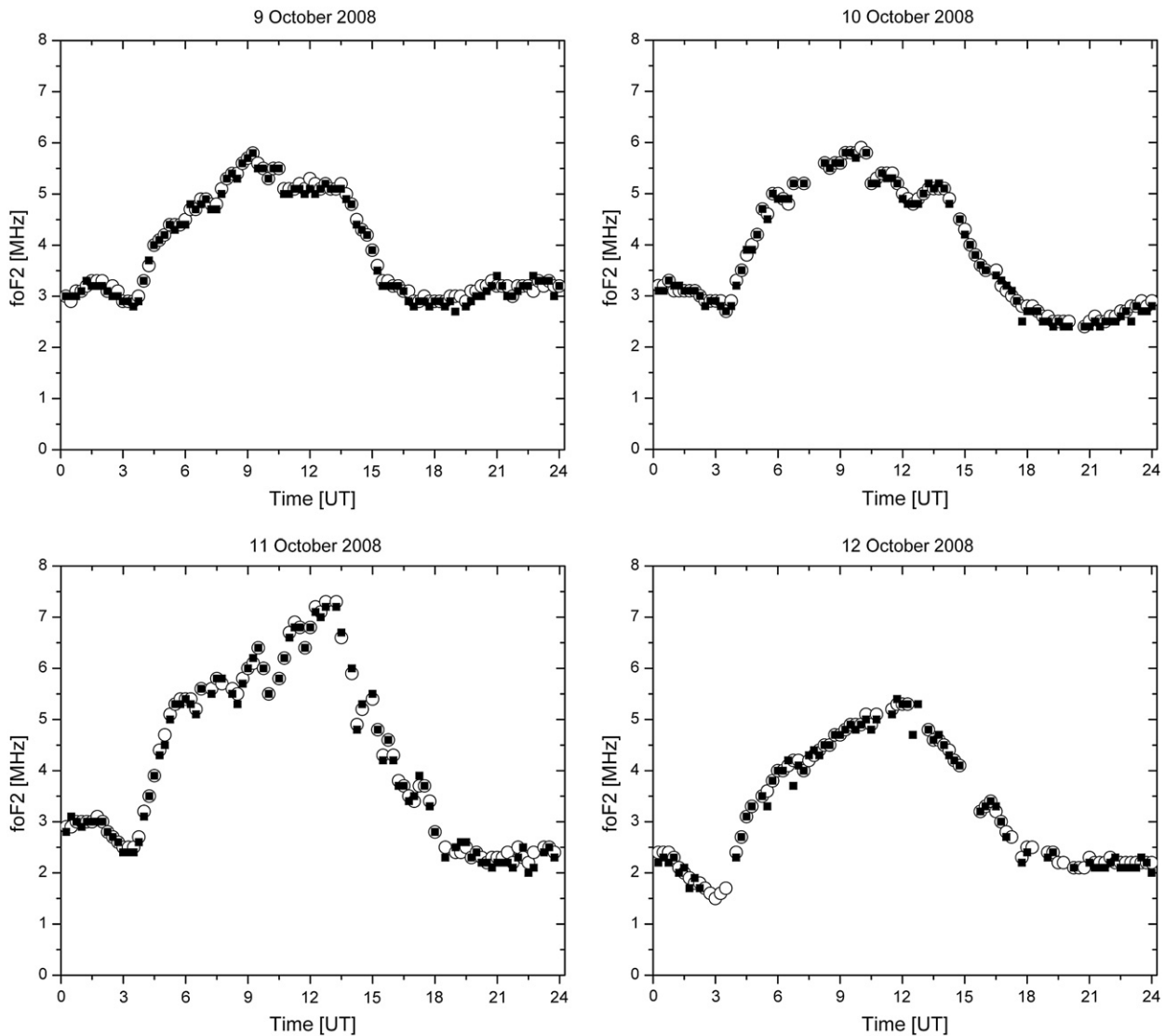


**Fig. 8.** 15 min  $foF2$  plots from 9 to 12 October 2008 as obtained from ionograms recorded by AIS-Parus ionosonde installed at Moscow. Values manually scaled from original ionogram files, and values obtained automatically by Autoscala from RDF ionogram files, are indicated by open circles, and solid squares, respectively.

Such a feature is related to the extrapolation process performed by Autoscala in case of the asymptotical vertical part (referring to F1 and F2 layers) or the final part (referring to the Es layer) of the trace are not well defined. This process introduces a slight underestimation of the automatically obtained critical frequency compared to the one manually scaled. It is worth noting that many ionograms of the dataset considered did not show the typical daytime trace, as illustrated in Fig. 4a. In this case the passage of a powerful travelling ionospheric disturbance, in the form of an internal acoustic-gravity wave (Cooper and Cummack, 1986; Krasheninnikov and Lianny, 1991), caused a modification of the electron density resulting in a break in the F2 mode trace and horizontal dishomogeneities that may be responsible for considerable focusing of a wave's field on some frequencies.

In addition, Fig. 6 shows an example of comparison between the electron density profile calculated by Autoscala and using the POLAN program (Titheridge, 1988). Three points deserve highlighting: (1)  $f_oF_2$  is slightly underestimated (0.1 MHz) by Autoscala and consequently it is the maximum of the electron density profile; (2) the E region valley calculated by Autoscala is overestimated; and (3) unlike Autoscala, POLAN starts estimating a topside electron density profile.

## 6. Performance for disturbed conditions: a case study

To test the quality of the software, and to assess whether the loss of information following the ionograms file transformation described in Section 2 could significantly affect Autoscala during disturbed conditions, ionograms from 9, 10, 11, and 12 October 2008 were considered. This is because, as illustrated in Fig. 7, on 11 October 2008 a strong geomagnetic storm occurred.

In Fig. 8 the 15 min  $f_oF_2$  values obtained manually from the original ionogram files are compared with the corresponding ones scaled by Autoscala from the RDF ionogram files. This sequence of daily plots shows that two quiet days are followed by a disturbed day (positive ionospheric phase), which in turn is followed again by a quiet day. Fig. 8 highlights how the whole sequence is well matched by Autoscala, giving evidence both that the algorithm has good results also for disturbed conditions and that the loss of information characterizing the ionogram file transformation does not affect the algorithm in a significant way.

## 7. Conclusions

The comparison between the results obtained automatically, and those obtained manually by a well-experienced scaler, showed that the system AIS-Parus & Autoscala provides acceptable automatically scaled values for a high percentage of ionograms. Further work is however necessary to improve the asymmetrical distributions of errors.

## References

- Cooper, J., Cummack, C.H., 1986. The analysis of travelling ionospheric disturbance with non-linear ionization response. *Journal of Atmospheric and Terrestrial Physics* 48 (1), 61–71.
- Gajdanskij, V.I., Karpenko, A.L., Krasheninnikov, I.V., Manaenkova, N.I., Silvestrov, S.V., Smirnov, A.A., 1996. The base network digital ionospheric station "Parus". In: *Proceedings XXVth General Assembly of the International Union of Radio Science*, Lille, France, Abstract 360.
- Krasheninnikov, I.V., Lianny, B.E., 1991. On interpretation of one kind of travelling ionospheric disturbance on  $vi$  ionograms. *Geomagnetism and Aeronomy* 31 (3), 427–433 in Russian.
- Pezzopane, M., 2004. *Interpre*: a Windows software for semiautomatic scaling of ionospheric parameters from ionograms. *Computer & Geosciences* 30, 125–130.
- Pezzopane, M., Scotto, C., 2004. Software for the automatic scaling of critical frequency  $f_oF_2$  and  $MUF(3000)F_2$  from ionograms applied at the ionospheric observatory of Gibilmanna. *Annals of Geophysics* 47 (6), 1783–1790.
- Pezzopane, M., Scotto, C., 2005. The INGV software for the automatic scaling of  $f_oF_2$  and  $MUF(3000)F_2$  from ionograms: a performance comparison with ARTIST 4.01 from Rome data. *Journal of Atmospheric and Solar Terrestrial Physics* 67 (12), 1063–1073.
- Pezzopane, M., Scotto, C., 2007. The automatic scaling of critical frequency  $f_oF_2$  and  $MUF(3000)F_2$ : a comparison between Autoscala and ARTIST 4.5 on Rome data. *Radio Science* 42 (RS4), 003, doi:10.1029/2006RS003581.
- Pezzopane, M., Scotto, C., 2008. A method for automatic scaling of F1 critical frequencies from ionograms. *Radio Science* 43 (RS2), S91, doi:10.1029/2007RS003723.
- Pezzopane, M., Scotto, C., Stanislawski, I., Juchnikowski, G., 2008. Autoscala applied at the ionospheric station of Warsaw. *INAG (Ionosonde Network Advisory Group) Bulletin*, 69.
- Scotto, C., 2009. Electron density profile calculation technique for Autoscala ionogram analysis. *Advances in Space Research* 44 (6), doi:10.1016/j.asr.2009.04.037.
- Scotto, C., Pezzopane, M., 2002. A software for automatic scaling of ionograms. In: *Proceedings of the XXVIIth General Assembly of the International Union of Radio Science*, Maastricht, The Netherlands, pp. 1018–1021.
- Scotto, C., Pezzopane, M., 2007. A method for automatic scaling of sporadic E layers from ionograms. *Radio Science* 42 (RS2), 012, doi:10.1029/2006RS003461.
- Scotto, C., Pezzopane, M., 2008. Removing multiple reflections from the F2 layer to improve Autoscala performance. *Journal of Atmospheric and Solar Terrestrial Physics* 70 (15), 1929–1934, doi:10.1016/j.jastp.2008.05.012.
- Titheridge, J.E., 1988. The real height analysis of ionograms: a generalised formulation. *Radio Science* 5, 831–849.